Desalination and Water Treatment
www.deswater.com

doi: 10.5004/dwt.2022.28234

263 (2022) 220–229
July

Understanding saline water dynamics in coastal aquifers using sand tank experiment and numerical modeling

Shahad Al-Yaqoubi[a,b,*], Ali Al-Maktoumi[a,c], Anvar Kacimov[a], Osman Abdalla[d], Mohammed Al-Belushi[a]

[a]*Soils, Water and Agricultural Engineering, College of Agricultural and Marine Sciences, Sultan Qaboos University, Oman, email: sm.alyaqooby94@gmail.com (S. Al-Yaqoubi)*
[b]*Oman Water Society, Oman*
[c]*Water Research Center, Sultan Qaboos University, Oman*
[d]*Earth Science, College of Sciences, Sultan Qaboos University, Oman*

Received 28 February 2022; Accepted 1 May 2022

ABSTRACT

A better understanding of seawater intrusion (SWI) problem in coastal aquifers is important for a perspicacious management of groundwater resources. SWI is affected by various hydrogeological and hydrological parameters such as: hydraulic conductivity (K_{sat}) of the aquifer, abstraction rate, recharge rate, density of seawater, etc. The objective of this paper is to explore saline water dynamics in an unconfined aquifer under different hydraulic gradients and under managed aquifer recharge (MAR) by using sand tank experiments and numerical simulations using SEAWAT code. Also, the efficiency of MAR in countering SWI malady was explored under different values of K_{sat} by using SEAWAT code. Numerical modeling is an effective tool to investigate the effect of K_{sat} on seawater dynamics. Modeling is cheaper and required less time as compared to the sand tank experiment. The sand tank experiment showed that the retreat rate of the saline water interface is always higher than the intrusion rate. As the hydraulic gradient across the sand tank increases, the saline water interface recedes further in the seaward direction. Injection of 1,060 cm^3 freshwater into a well located at the toe of a saline water interface caused its retreat seaward by 40%. The calibrated model was used to simulate the effect of aquifer's hydraulic conductivity on the dynamics of saline water under MAR. The results show that MAR practiced in highly conductive aquifers was less effective in combatting SWI because the injected water discharges rapidly from the aquifer. A small water table mound develops when MAR is practiced in a highly conductive porous medium and hence there is only a small effect in controlling SWI. In contrast, a low aquifer's hydraulic conductivity slows down water flow, develops a higher water table mound and thus induces a significant effect on controlling SWI. Therefore, optimizing MAR requires close consideration of geological settings and hydrological conditions to ensure high efficiency of MAR in mitigation of salinized aquifer.

Keywords: Managed aquifer recharge; Injection wells; Seawater intrusion; Sand tank experiment; SEAWAT

1. Introduction

Groundwater is the main source of freshwater in arid regions that are characterized by limited water resources due to the low rate of precipitation. More stresses are exerted on coastal groundwater aquifers due to expansion of freshwater demand by municipalities, industries, agriculture, aggravated by the population growth [1,2]. Management of coastal aquifers is of high importance to sustain its usability for water supply. One of the main threats to degradation

* Corresponding author.

Presented at the 14th Gulf Water Conference: Water in the GCC… Towards Economic Efficiency and Financial Sustainability, 13–15 February 2022, Riyadh, Saudi Arabia

of water quality in coastal aquifers is seawater intrusion (SWI). SWI is the invasion of saline water into coastal aquifers [3,4]. The difference between freshwater and saline water specific gravity induces the ingression of the seawater into the aquifers [5]. SWI is classified into two types which are active and passive. Active SWI occurs when the hydraulic gradient in the aquifer is reversed to be in the landward direction whereas passive SWI occurs, when the hydraulic gradient is oriented seaward but of small value that is not enough to control SWI [6–8]. In our study presented here, we consider the case of passive SWI. In many coastal aquifers (especially, in arid regions), SWI is accelerated by over-abstraction of fresh groundwater and limited natural recharge. In fact, mismanagement of coastal aquifers accelerates the deterioration of the groundwater. The rate at which SWI occurs in a coastal aquifer depends on the abstraction rate, depth and intervals of the screens of abstraction wells, the concentration of salts in groundwater, and the hydraulic gradient among other factors [9]. Other hydrological parameters that affect the rate of SWI are K_{sat} of the geological formation of the aquifer, aquifer's geometry, density ratio (seawater/freshwater), and boundary conditions [10]. SWI is also affected by sea-level rise due to climate change, or in some areas due to land subsidence [8,11,12]. Tidal fluctuation may affect the scale of intrusion within the intertidal zone [13,14]. SWI can be controlled by implementation of physical barriers such as subsurface dams, cut-off walls, and mixed physical barriers [15,16], as well as hydraulic barriers such as negative (abstraction well), positive (injection well), and mixed barriers (abstraction and injection wells) [5]. Also, SWI can decelerate by using managed aquifer recharge (MAR), controlling the abstraction rate [17] and pumping from the transition zone [18]. MAR is shown to manage and protect coastal aquifers and slow down the SWI rate [19,20]. SWI was studied by sand tank experiments [2,9,21–29], analytical modeling [10,28,30–35] and numerical modeling [24,25,27,36,37]. The objective of this paper is twofold:

- Study the impact of different hydraulic gradients and MAR (by injection wells) on the dynamics of the saline water interface by using sand tank experiment.
- Numerically study the impact of K_{sat} on the efficiency of MAR in countering SWI problem.

2. Laboratory methods

2.1. Details of the experimental set-up

The sand tank utilized in this experiment was designed and fabricated using 2 mm thick transparent acrylic sheets. It is a rectangular parallelepiped with dimensions 100 cm long, 60 cm height and 15 cm wide (Fig. 1). The sand tank design considered the following aspects: the hydraulic gradient, the boundary conditions, the way the tank will be packed with soil and easiness of parameters measurement and data collection. The tank was packed using the wet-packing method where water is first added to the tank, followed with placing the selected sand material to avoid occurrence of a trapped air [2,26]. An artificial white coarse sand was used as a porous medium. The physical and hydrological properties of the sand were estimated in the lab. The grain diameter is 0.6 mm, the porosity (n) is 0.45 and K_{sat} is 4.5 cm/min. The tank is designed to have a water compartment at the left side to represent the upstream boundary (of freshwater), and another compartment at the downstream boundary (right side of the tank) to represent the seawater boundary. The two compartments are equipped with control valves that allow the selection of different hydraulic gradients across the tank corresponding to different runs. The inner walls of the compartments and the bottom boundary of the tank are lined with fine mesh to hold the packed soil and prevent colmation of drain valves. Two tanks of fifty-gallon capacity connected to the sand tank to supply both freshwater and artificially made saline water. The water is injected into the sand tank using two pumps (WP-7000: AC 220–240 V, 105 W, 50/60 Hz,). Liquid flow controller (Model: DFC15, DIGITEN) was used to measure and control the flow rate and to know the volume of both saline water and freshwater supplied into the sand tank during the experiment. The discharging water across both boundaries was measured during the experiment. The density of freshwater used during the experiments is 1.000 g/cm^3 and that for the saline water is 1.045 g/cm^3 (the salt's concentration is 50 g/L). To reach this concentration of saline water, around 14,000 g of table salt was dissolved in 180 L of freshwater.

The rate of intrusion and the length of saline water interface during all runs were measured by rulers (Fig. 1)

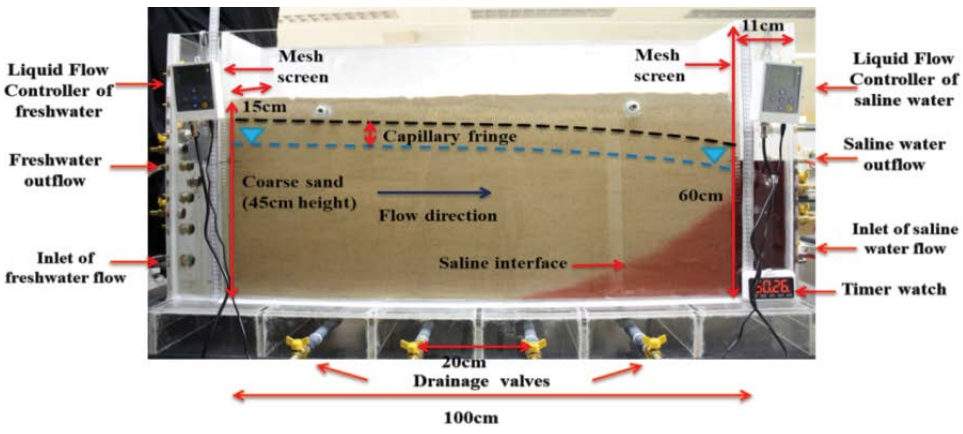

Fig. 1. Design of the sand tank.

and analysis of photos taken by a digital camera. The saline water was colored with Red Food Dye to easily visualize the movement of the saline water interface in the sand tank.

2.2. Procedure of different hydraulic gradient experiment

Different hydraulic gradients (i) were used to investigate the dynamics of the saline water interface. The interface advances and retreats backwards to the right compartment in Fig. 1. This oscillating behavior of the interface was measured using rulers fixed along the bottom side of the tank and along the vertical seawater boundary. The saline water interface toe (X_{toe}) position, depth to the interface at x = 0 (the coastline) (z_w), the discharge zone (DZ), and the seepage face (SF) were recorded during all runs. The inflow rate of freshwater into the tank was measured (using a flow rate controller) to be about 2.5 L/min while saline water supplied into the tank at the rate of 1.5 L/min. The experiments run until the system reach steady-state conditions at which the saline water interface stabilizes. The results were compared when the system reaches steady-state. The system considered reaching steady-state when (X_{toe}) position does not change with time. The parameters for all runs in this experiment are summarized in Table 1.

2.3. Procedure of injection well experiment

One injection well was fixed at the middle of the sand tank (50 cm from the saline water compartment) and at 42 cm depth from the top of the porous medium. The diameter of an injection well was 2 cm. The injection freshwater was colored with a blue food dye. Also, the level of the water table was monitored and measured using water level sensors. The injection started when the X_{toe} reached 50 cm from the seawater boundary. In addition, the areas cleaned from the saline water for all laboratory sand-tank experiments were calculated using Mathematica5 program. Also, the pore volume of area cleaned from saline water was calculated by Eq. (1) [38]. The injected volume of freshwater needed to reduce the salinity of a certain area of the aquifer that is contaminated by saline water was also evaluated.

$$\text{Pore volume} = \begin{pmatrix} \text{Vertical cross section area} \\ \times \text{Length of the tank} \end{pmatrix} \times \text{porosity} \quad (1)$$

2.4. Numerical modeling approach

MAR laboratory experiment was simulated using the SEAWAT code (MODFLOW Processing Pro version 8.0.31, Simcore software [39]). This code was run for steady-state conditions. The conceptual model used is presented in Fig. 2. The dimensions of modeled domain are x = 100 cm and y = 30 cm. The modeled domain was discretized with a grid size of Δy and Δx = 1 cm based on grid sensitivity analysis [40]. We assigned constant heads for both saline and freshwater boundaries and assigned a no-flow boundary for the bottom of the rectangle in Fig. 2. The parameters used in

Table 1
Parameters used for different hydraulic gradient experiment

No. of runs	Constant head of freshwater (h_f) (cm)	Constant head of saline water (h_s) (cm)	i = (dh/dl)	Inflow rate of freshwater (L/min)	Inflow rate of saline water (L/min)	Concentration of inlet saline water (g/L)
1	23	22.6	0.004	2.5	1.5	50
2	23	20.6	0.024	2.5	1.5	50
3	30.5	29.7	0.008	2.5	1.5	50
4	30.5	27.5	0.03	2.5	1.5	50
5	30.4	27.8	0.026	2.5	1.5	50
6	34	27.8	0.062	2.5	1.5	50

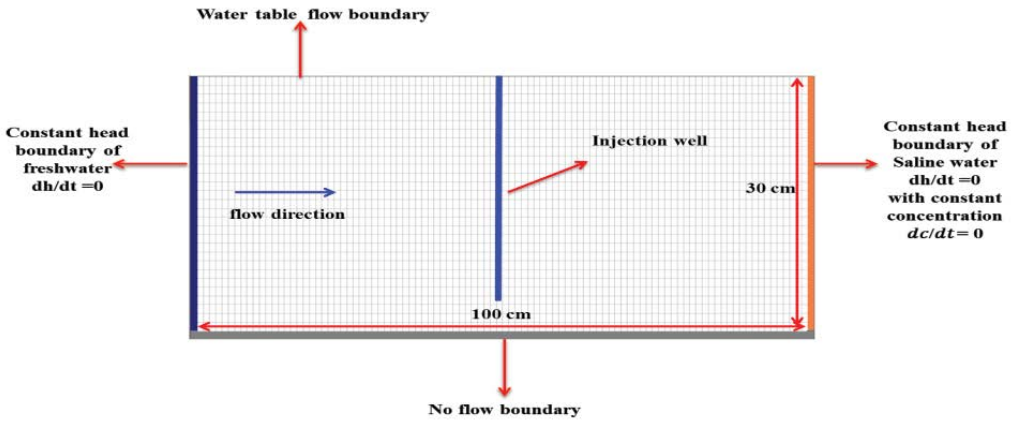

Fig. 2. Sketch of conceptual model for SEAWAT simulations.

simulations are presented in Table 2. Trial and error method was used for calibration. After calibration, SEAWAT was used to simulate our sand tank experiment, and to explore the impact of K_{sat} on the dynamics of saline water interface under MAR. Numerical modeling is a good tool to explore variation of parameters. Simulations are much cheaper compared with physical experiments. There are less associated efforts and sources of uncertainty, which are inevitable in physical experiments, for example, during packing and unpacking of porous media. Selected iso-concentric lines (isochlors) were plotted and used for comparison purposes.

3. Results and discussion

3.1. Dynamics of saline water interface under different hydraulic gradients

The effect of the hydraulic gradient (i) on the dynamics of the saline water interface was investigated. Fig. 3a presents the results of Run 1 for i = 0.004. The (h_f) and (h_s) were kept at 23 and 22.6 cm, respectively. In this run, during the first 5 min, X_{toe} advanced 6 cm upstream. Then the rate at which the saline water interface migrated in the tank towards the freshwater compartment was 1.4 cm/min. The rate decelerated with time is 0.1 cm/min (Fig. 4a). In average, the saline water interface intruded with the rate of (0.134 cm/min) during the 530 min of the experiment before reaching steady-state (Fig. 4a). The total inflow of freshwater into the tank during this experiment (until the steady-state condition reached, 530 min) was 600 L (600,000 cm^3) and 350 L (350,000 cm^3) of saline water intruded. The X_{toe} reached almost the upstream boundary. The z_w was 19.5 cm, DZ was 5.5 cm, and SF was 4.5 cm (Fig. 3a). During this run, the saline water contaminated about 7,590.4 cm^3 of the aquifer volume (the total aquifer volume in the tank considering 23 cm depth and 15 cm inner width for the porosity of 0.45 is 15,525 cm^3). The metered freshwater discharge (q_{out}) (at steady-state) through the coastal boundary was 1.5 L/min (1,500 cm^3/min) (Fig. 5) with concentration of 48 g/L. In Run 2 (Fig. 3b), i was 0.024 and the retreat of the saline water interface from its position in Run 1 (99 cm upstream the coastal boundary) was monitored and evaluated. The h_f and h_s were set to 23 and 20.6 cm, respectively. The interface receded back (right part in Fig. 3b) at an average rate of 0.33 cm/min during the first 245 min. The interface stabilized (reached steady state) after 245 min (Fig. 4b) and X_{toe} was at 11 cm from the coastal boundary. The changed values of z_w, DZ, and SF are shown in Fig. 3b. Setting i to 0.024 caused a retreat of the interface by about 88 cm. During this run, a total volume of inflowing freshwater into the tank across the upstream boundary measured as 520 L (520,000 cm^3) while the intruded saline water through the coastal boundary was 300 L (300,000 cm^3). The aquifer pore volume occupied by saline water was 380.3 cm^3 which is equivalent to 5% only of the aquifer volume. We found that a total inflow of 520 L (520,000 cm^3) of freshwater cleaned about 1,068.17 cm^2 of salinized area of the aquifer which is equivalent to 7,210.2 cm^3 of the pore volume. The q_{out} (at steady-state) through the seawater boundary was 1.5 L/min and the concentration of the discharged water was 46 g/L (Fig. 5).

In the third run, the hydraulic gradient was reduced again to allow intrusion but under the hydraulic gradient higher than that used in Run 1. The new i is 0.008 (h_f and

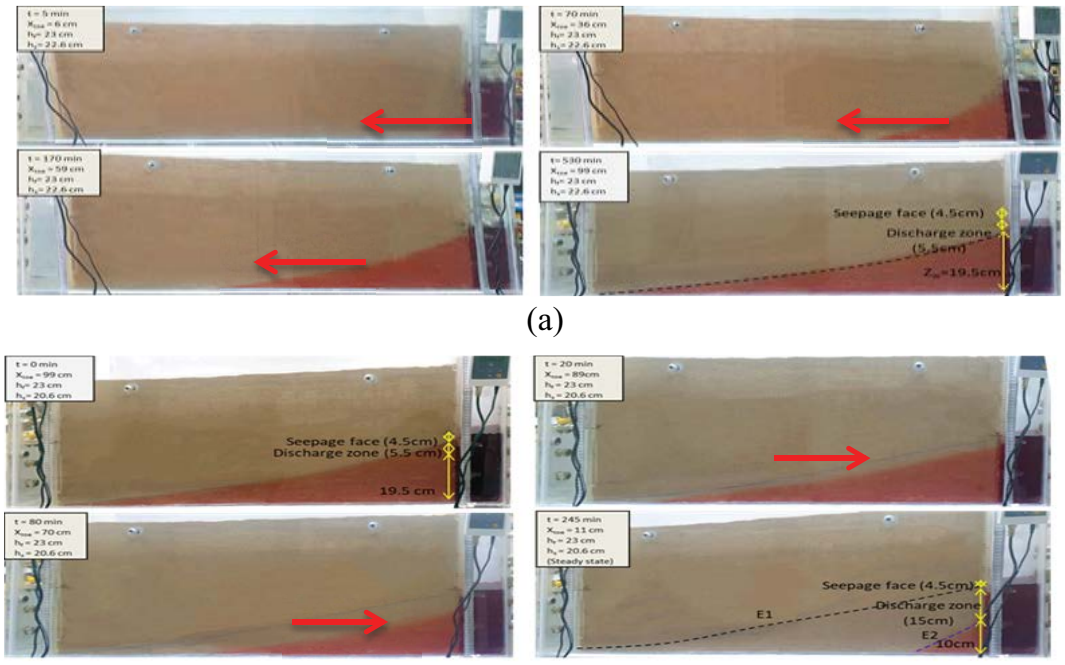

Fig. 3. Photos for (a) Run 1: SWI at selected times (5, 70, 170, and 530 min) for i of 0.004 and (b) Run 2: seawater retreat at selected times (0, 20, 80, and 245 min) for i of 0.024 when i was reset to 0.024 instead of 0.004.

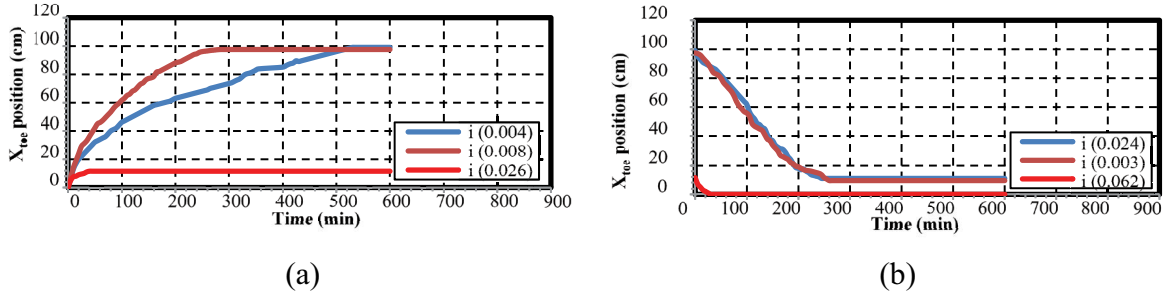

Fig. 4. Summary of the effect of i in saline water intrusion over time considering X_{toe}: (a) saline water intrusion and (b) saline water retreat.

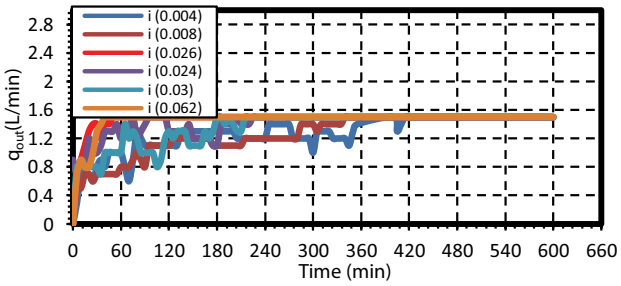

Fig. 5. Freshwater discharge q_{out} through seawater boundary.

h_s set to 30.5 and 29.7 cm, respectively). The ingression of the saline water interface is presented in Fig. 6a. The saline water interface moved faster at the beginning with a rate of 1.4 cm/min during the first 10 min (X_{toe} reached 14 cm inland). Then, the rate gradually decreased to 0.002 cm/min (Fig. 4a). The saline water interface intruded forwards with an average rate of 0.1051 cm/min during 285 min after which the system stabilized when the X_{toe} was at 97.5 cm. During this run, a total of 590 L (590,000 cm^3) of freshwater flow into the tank from the upstream boundary while an amount of 330 L (330,000 cm^3) was the inflow to the tank from the seawater boundary. The corresponding values of z_w, DZ and SF were 25.5, 5, and 6 cm, respectively (Fig. 6a). The salinized aquifer volume under i = 0.008 is 7,527.5 cm^3 which is almost similar to that of Run 1 for gradient of 0.004 (7,590 cm^3) and 20 times more than that for gradient of 0.024. The q_{out} via the seawater boundary at steady state was similar to that measured for i = 0.024 (1.5 L/min) with the concentration of the discharged water of 47.8 g/L (Fig. 5). Fig. 6b shows the results of Run 4 for i = 0.03 (h_f and h_s were 30.5 and 27.5 cm, respectively). The values of h_f and h_s are selected based on the pre-existing control valves. Analyses of the data are presented in Fig. 4b, shows that the saline water interface receded back with an average rate of 0.1214 cm/min during the first 260 min after which the flow reached steady state. The X_{toe} was measured to be at 9.5 cm from the coastal boundary. The z_w, and SF decreased to 10 and 3 cm, respectively, and DZ increased to 17.5 cm (Fig. 6b). For the X_{toe} to retreat by 88 cm (from where it was at i = 0.008) to the steady-state at i = 0.03, around 500 L (500,000 cm^3) of freshwater flushed the tank over the 260 min. However; an inflow of 230 L (230,000 cm^3) of saline water only entered the aquifer through the coastal boundary. In general, as i increases the SWI decreases as the freshwater flow acts against the landward ingression of the interface. This is in fact agreeing with the findings in the literature.

Fig. 7a shows Run 5 with i = 0.026 (h_f and h_s are 30.4 and 27.8 cm, respectively). The saline water interface intruded over a distance of 11.5 cm with an average rate of (0.0321 cm/min) over a period of 40 min at which the system reached an equilibrium state (Fig. 4a). Also, z_w, DZ and SF were found to be 11, 17.5, and 3 cm, respectively, Fig. 7a. The occupied volume by saline water was 440.7 cm^3. When the equilibrium state reached in Run 5, the hydraulic gradient in the tank during Run 6 increased to 0.062 (the h_f and h_s were 34 and 27.8 cm, respectively). As a result, the interface retreated towards the saline water compartment with an average rate of 0.1516 cm/min over 25 min. The saline water flushed out completely from the system after 25 min (Figs. 4b and 7b). About 35 L (35,000 cm^3) of freshwater flushed out through the tank and resulted in cleaning out 440.7 cm^3 of salinized aquifer volume. The flow rate q_{out} for all runs at steady-state was practically the same (1.5 L/min). However, the concentration of discharging water varied, depending on the i value. For Runs 5 and 6, q_{out} is presented in Fig. 5 and the concentration of outflowing water was 46 and 40 g/L, respectively.

The results in Fig. 4a and b show that the retreat rate of the interface is always faster than the intrusion rate. This finding is similar to what is found by experiments of Goswami and Clement [24] and analytical solution by Rathore et al. [10]. From the curve in Fig. 8, it seems that the relation between i values and the X_{toe} is not simply linear. It seems that there is a threshold value of i beyond which the change in the position is not really significant. This means that after certain i value, the induced effect on the position of the interface is negligible. As that, flushing out the aquifer with a larger volume of freshwater will be just a waste.

3.2. Experimenting with the dynamics of saline water interface under MAR injection well

The injection well located at 50 cm from seawater boundary (Run 7). Injection of 1.06 L (1,060 cm^3) of freshwater causes retreat of the X_{toe} in the seaward direction by 20 cm (X_{toe} reached 30 cm from the seawater boundary (retreated by 40%)). The shape of the saline water interface

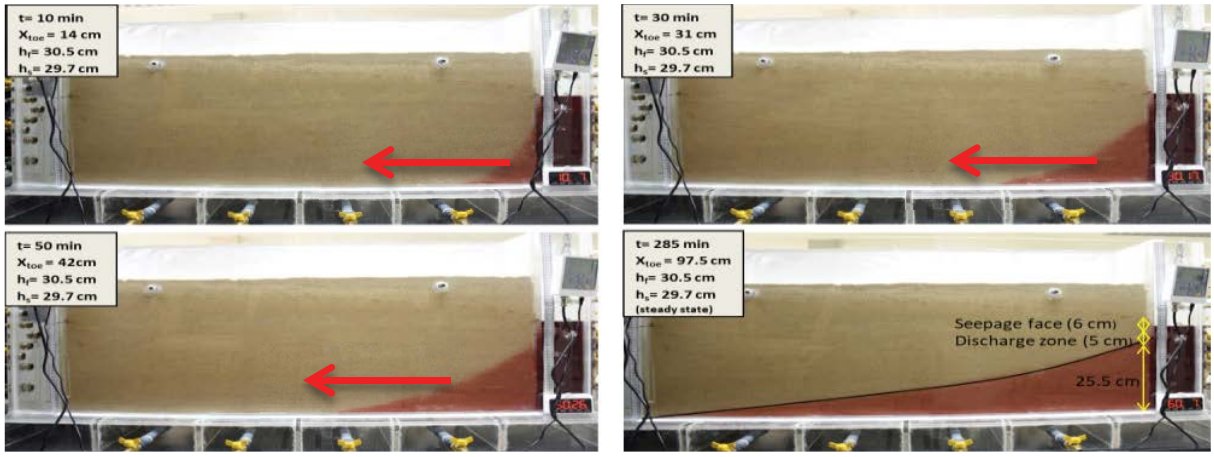

(a)

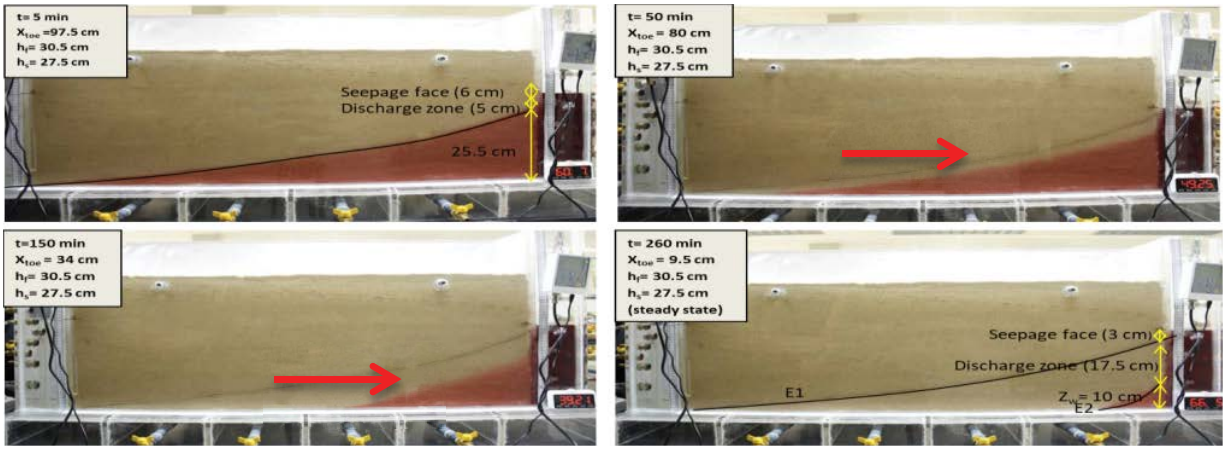

(b)

Fig. 6. Photos for (a) Run 3: SWI at selected times (10, 30, 50 and 285 min) under *i* of 0.008 and (b) Run 4: seawater retreat at selected times (5, 50,150 and 260 min) under *i* of 0.03 when was reset to 0.03 instead of 0.008.

Table 2
SEAWAT parameters for the base case run

Parameter	Value	Parameter	Value
Hydraulic head at freshwater boundary	23.0 (cm)	Courant number	0.5 (–)
Hydraulic head at saline water boundary	22.6 (cm)	Longitudinal dispersivity	0.1 (cm)
K_{sat}	4.5 (cm/min)	Diffusion coefficient	0.5 cm^2/min
Effective porosity	0.45 (–)	Seawater concentration	50 (g/L)

is affected by the MAR. The X_{toe} is at 30 cm, z_w of 17.5 cm and the thickness of the interface at 25 cm from the coastal boundary (z_x) is 7.5 cm (Fig. 9a and b). The salinized area before injection was found to be 479.652 cm^2. Injection of around 1.06 L of freshwater cleaned around 173.60 cm^2 of this salinized zone. The pore volume of the cleaned area is calculated as 1,171.8 cm^3.

3.3. Numerical simulation to investigate the effect of the hydraulic conductivity of the aquifer on SWI

Steady state calibration of the developed model was performed (for the experimental Run 7 discussed above). A good agreement between the results obtained from the numerical simulations and the sand tank experiment was

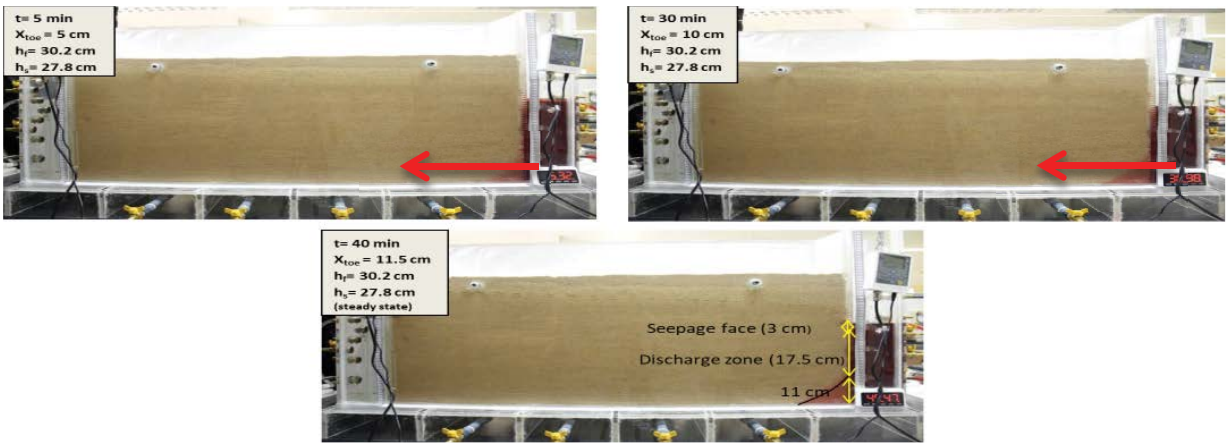

(a)

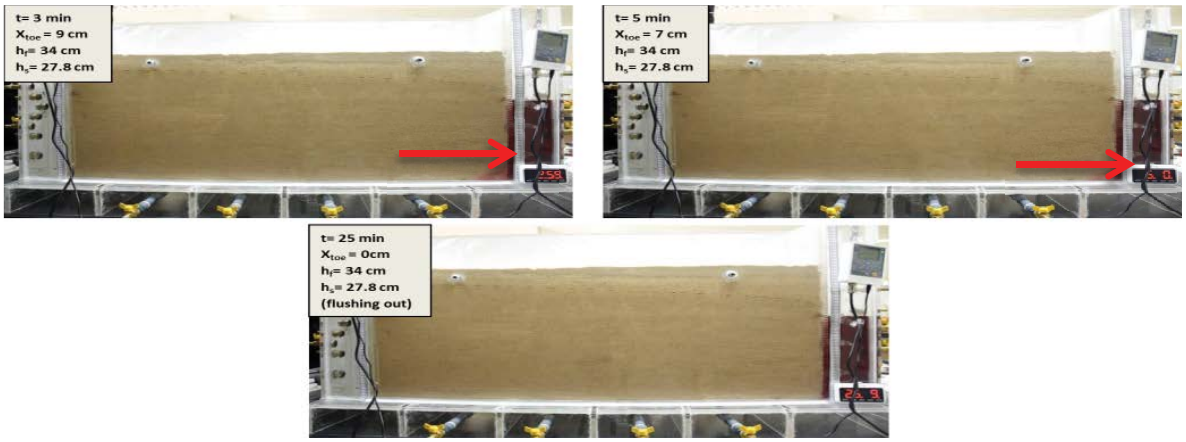

(b)

Fig. 7. Photos for (a) Run 5: SWI at selected times (5, 30 and 40 min) under *i* of 0.026 and (b) Run 6: seawater retreat at selected times (3, 5 and 25 min) under *i* of 0.062 when *i* reset to 0.062 instead of 0.026.

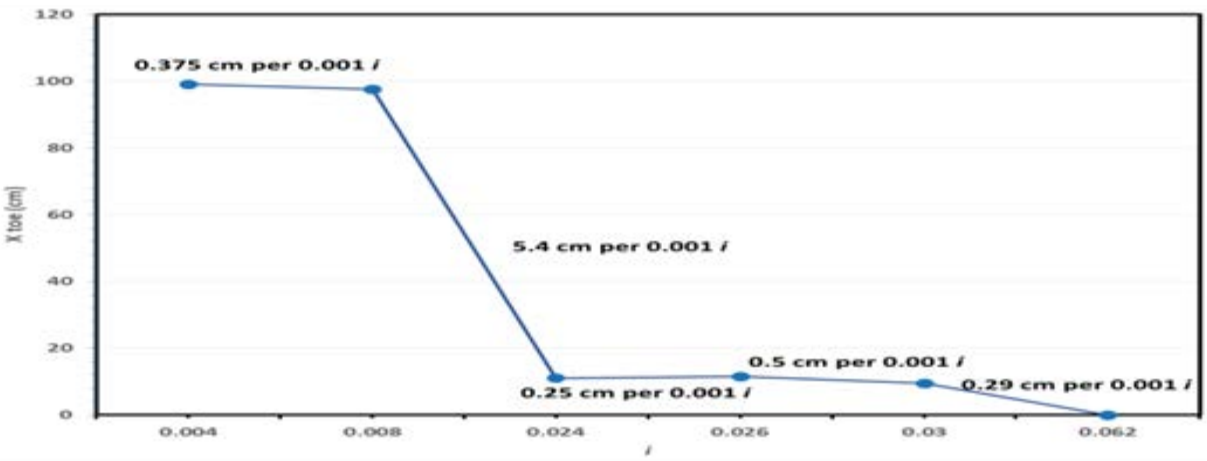

Fig. 8. Position X_{toe} under different *i*.

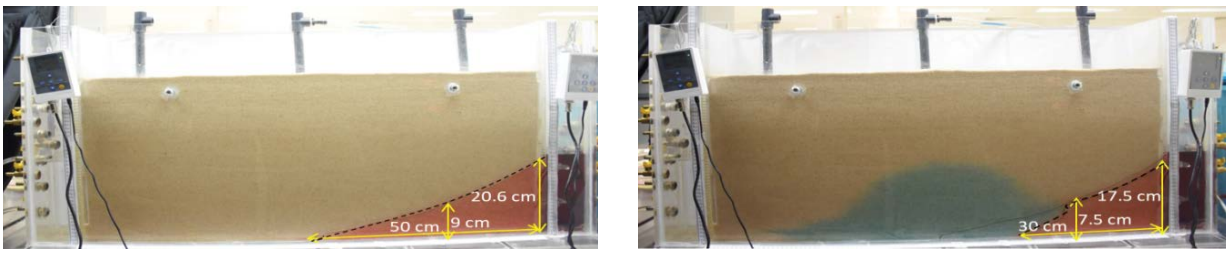

Fig. 9. Saline water interface: (a) before injection and (b) during injection (after 15 min since commencement of injection).

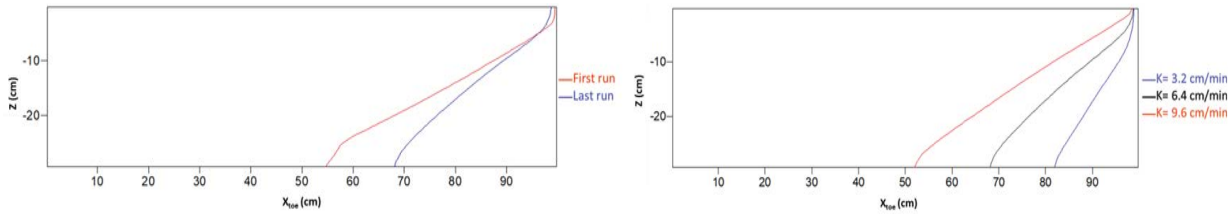

Fig. 10. (a) X_{toe} position modeled as 70% isochlor (during injection) for the first and final calibration and (b) 70% isochlor under different values of K during injection.

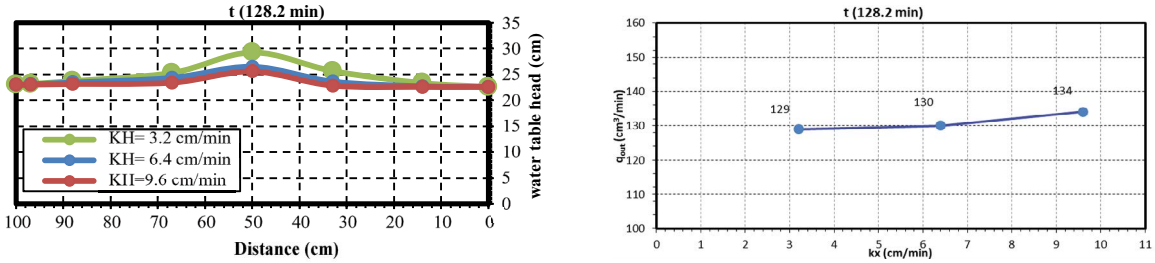

Fig. 11. (a) Water table height for different K_{sat} values and (b) simulated q_{out} volume for the simulations for different K_{sat}.

found for the following parameter set (porosity = 0.56, K_{sat} 6.4 cm/min, the initial longitudinal dispersivity ($\propto_L$) = 2.5 cm and the diffusion coefficient = 0.007 cm^2/min). Under injection, X_{toe} retreated from 50 to 31 cm from the seawater boundary (retreated by 38%) (Fig. 10a) which is very close to X_{toe} during the sand tank experiment (Fig. 9b). High permeability of the aquifer caused a high rate of SWI that agrees with Abdoulhalik and Ahmed [41]. The calibrated model was used to investigate the impact of K_{sat} on the dynamics of the interface under the injection at the toe position. The K_{sat} values of 3.2, 6.4, and 9.6 cm/min, were examined. X_{toe} prior to injection was 50 cm. First, during injection of 1,060 cm^3 under K_{sat} value of 6.4 cm/min, the X_{toe} of the selected 70% isochlor retreated by 19 cm seawards. Then, K_{sat} was increased to 9.6 cm/min, and X_{toe} receded backward by only 2 cm. However, when K_{sat} value decreased to 3.2 cm/min, the X_{toe} retreated by 32 cm (from 50 to 18 cm, by 64%) (Fig. 10b). The height of the water table mound was larger under a smaller K_{sat} value (Fig. 11a). Analysis of the water budget in the numerical simulations showed that injection into a low permeable material resulted in less discharge of water outside the tank (Fig. 11b). Hence, the developed water table mound was high and induced more effect on the interface (the interface retreats further seawards). In general, the simulations illustrated that K_{sat} is one of the key factors for MAR to induce significant effect in controlling SWI.

4. Conclusion

This paper presents the results of sand tank experiments and numerical modeling to investigate the dynamics of SWI in a coastal aquifer under MAR activities for different hydraulic properties of the aquifer. The feasibility of MAR in SWI mitigation was assessed and the rate of interface retreatment was found faster than the rate of its advancement. The sand tank experiment illustrates the importance of the gradient i in controlling SWI. SEAWAT simulations manifested that low aquifer's hydraulic conductivity increases the effectiveness of MAR in controlling SWI. If MAR practiced in highly conductive porous medium, the impact of the injection on controlling SWI is low. This is because of a rapid discharge of injected water out of the aquifer. In very permeable aquifers, the height of the developed water table mound is relatively small that

limits induced piezometric heads needed for a seaward push of the saline water interface. Sand tank experiments and numerical modeling should be extended to consider heterogeneous aquifers and other hydrological drivers, like the abstraction rate of groundwater, and parameters of tidal fluctuations at the sea boundary.

Acknowledgements

The first author acknowledges the assistance of the administration of Sultan Qaboos University (SQU) in awarding her a full MSc scholarship. The authors would like to further extend acknowledgement to the financial support provided by SQU through internal grant IG/AGR/SWAE/19/01 and the support of the Research Group DR/RG/17.

References

[1] A.R. Kacimov, M.M. Sherif, Sharp interface, one-dimensional seawater intrusion into a confined aquifer with controlled pumping: analytical solution, Water Resour. Res., 42 (2006), doi: 10.1029/2005WR004551.
[2] S. Sadjad Mehdizadeh, F. Vafaie, H. Abolghasemi, Assessment of sharp-interface approach for saltwater intrusion prediction in an unconfined coastal aquifer exposed to pumping, Environ. Earth Sci., 73 (2015) 8345–8355.
[3] J. Bear, A.H.-D. Cheng, S. Sorek, D. Ouazar, I. Herrera, Seawater Intrusion in Coastal Aquifers: Concepts, Methods and Practices, Vol. 14, Springer Science & Business Media, Dordrecht, 1999.
[4] S. Maury, S. Balaji, Application of resistivity and GPR techniques for the characterization of the coastal litho-stratigraphy and aquifer vulnerability due to seawater intrusion, Estuarine Coastal Shelf Sci., 165 (2015) 104–116.
[5] M. Pool, J. Carrera, Dynamics of negative hydraulic barriers to prevent seawater intrusion, Hydrogeol. J., 18 (2010) 95–105.
[6] S. Badaruddin, A.D. Werner, L.K. Morgan, Characteristics of active seawater intrusion, J. Hydrol., 551 (2017) 632–647.
[7] A.D. Werner, On the classification of seawater intrusion, J. Hydrol., 551 (2017) 619–631.
[8] A.D. Werner, M. Bakker, V.E.A. Post, A. Vandenbohede, C. Lu, B. Ataie-Ashtiani, C.T. Simmons, D.A. Barry, Seawater intrusion processes, investigation and management: recent advances and future challenges, Adv. Water Resour., 51 (2013) 3–26.
[9] S. Noorabadi, A.H. Nazemi, A.A. Sadraddini, R. Delirhasannia, Laboratory investigation of water extraction effects on saltwater wedge displacement, Global J. Environ. Sci. Manage., 3 (2017) 21–32.
[10] S.S. Rathore, Y. Zhao, C. Lu, J. Luo, Analytical analysis of the temporal asymmetry between seawater intrusion and retreat, Adv. Water Resour., 111 (2018) 121–131.
[11] C. Lu, P. Xin, L. Li, J. Luo, Seawater intrusion in response to sea-level rise in a coastal aquifer with a general-head inland boundary, J. Hydrol., 522 (2015) 135–140.
[12] S. Sadjad Mehdizadeh, S.E. Karamalipour, R. Asoodeh, Sea level rise effect on seawater intrusion into layered coastal aquifers (simulation using dispersive and sharp-interface approaches), Ocean Coastal Manage., 138 (2017) 11–18.
[13] B. Ataie-Ashtiani, R.E. Volker, D.A. Lockington, Tidal effects on seawater intrusion in unconfined aquifers, J. Hydrol., 216 (1999) 17–31.
[14] W.K. Kuan, G. Jin, P. Xin, C. Robinson, B. Gibbes, L. Li, Tidal influence on seawater intrusion in unconfined coastal aquifers, Water Resour. Res., 48 (2012), doi: 10.1029/2011WR010678.
[15] A. Abdoulhalik, A. Ahmed, G.A. Hamill, A new physical barrier system for seawater intrusion control, J. Hydrol., 549 (2017) 416–427.
[16] Y. Ru, K. Jinno, T. Hosokawa, K. Nakagawa, Study on Effect of Subsurface Dam in Coastal Seawater Intrusion, First International Conference on Saltwater Intrusion and Coastal Aquifers—Monitoring, Modeling, and Management, Essaouira, Morocco, April 23–25, 2001.
[17] I. Siarkos, D. Latinopoulos, Z. Mallios, P. Latinopoulos, A methodological framework to assess the environmental and economic effects of injection barriers against seawater intrusion, J. Environ. Manage., 193 (2017) 532–540.
[18] M.M. Sherif, K.I. Hamza, Mitigation of seawater intrusion by pumping brackish water, Transp. Porous Media, 43 (2001) 29–44.
[19] A. Al-Maktoumi, M. El-Rawy, S. Zekri, O. Abdalla, Managed Aquifer Recharge Using Treated Wastewater to Mitigate Seawater Intrusion Along the Jamma Coastal Aquifer, Oman, International Congress of the International Water Association, Presented at the International Congress of the International Water Association, Amman, Jordan, 2015.
[20] G.Y. Ebrahim, A. Jonoski, A. Al-Maktoumi, M. Ahmed, A. Mynett, Simulation-optimization approach for evaluating the feasibility of managed aquifer recharge in the Samail lower catchment, Oman, J. Water Resour. Plann. Manage., 142 (2015) 05015007.
[21] A. Abdoulhalik, A.M. Abdelgawad, A.A. Ahmed, Impact of layered heterogeneity on transient saltwater upconing in coastal aquifers, J. Hydrol., 581 (2019) 124393, doi: 10.1016/j.jhydrol.2019.124393.
[22] A. Botero-Acosta, L.D. Donado, Laboratory scale simulation of hydraulic barriers to seawater intrusion in confined coastal aquifers considering the effects of stratification, Procedia Environ. Sci., 25 (2015) 36–43.
[23] S.W. Chang, T.P. Clement, Experimental and numerical investigation of saltwater intrusion dynamics in flux-controlled groundwater systems, Water Resour. Res., 48 (2012), doi: 10.1029/2012WR012134.
[24] R.R. Goswami, T.P. Clement, Laboratory-scale investigation of saltwater intrusion dynamics, Water Resour. Res., 43 (2007), doi: 10.1029/2006WR005151.
[25] R. Luyun Jr., K. Momii, K. Nakagawa, Laboratory-scale saltwater behavior due to subsurface cutoff wall, J. Hydrol., 377 (2009) 227–236.
[26] R. Luyun Jr., K. Momii, K. Nakagawa, Effects of recharge wells and flow barriers on seawater intrusion, Groundwater, 49 (2011) 239–249.
[27] S. Noorabadi, A.A. Sadraddini, A.H. Nazemi, R. Delirhasannia, Laboratory and numerical investigation of saltwater intrusion into aquifers, J. Mater. Environ. Sci., 8 (2017) 4273–4283.
[28] O.D.L. Strack, L. Stoeckl, K. Damm, G. Houben, B.K. Ausk, W.J. de Lange, Reduction of saltwater intrusion by modifying hydraulic conductivity, Water Resour. Res., 52 (2016) 6978–6988.
[29] S. Sugio, K. Nakada, D.W. Urish, Subsurface seawater intrusion barrier analysis, J. Hydraul. Eng., 113 (1987) 767–779.
[30] C. Lu, A.D. Werner, Timescales of seawater intrusion and retreat, Adv. Water Resour., 59 (2013) 39–51.
[31] X. Zhou, A method for estimating the fresh water–salt water interface with hydraulic heads in a coastal aquifer and its application, Geosci. Front., 2 (2011) 199–203.
[32] A.D. Koussis, K. Mazi, G. Destouni, Analytical single-potential, sharp-interface solutions for regional seawater intrusion in sloping unconfined coastal aquifers, with pumping and recharge, J. Hydrol., 416 (2012) 1–11.
[33] A.H.-D. Cheng, D. Halhal, A. Naji, D. Ouazar, Pumping optimization in saltwater-intruded coastal aquifers, Water Resour. Res., 36 (2000) 2155–2165.
[34] E.O. Frind, Seawater intrusion in continuous coastal aquifer-aquitard systems, Adv. Water Resour., 5 (1982) 89–97.
[35] M.A. Hashish, M.E. Rasmy, A.M. Amer, One-dimensional steady state seawater intrusion in leaky aquifers, Adv. Water Resour., 4 (1981) 34–42.
[36] A. Abdoulhalik, A.A. Ahmed, Transient investigation of saltwater upconing in laboratory-scale coastal aquifer, Estuarine Coastal Shelf Sci., 214 (2018) 149–160.
[37] S.W. Chang, T. Prabhakar Clement, Laboratory and numerical investigation of transport processes occurring above and within a saltwater wedge, J. Contam. Hydrol., 147 (2013) 14–24.
[38] C.W. Fetter, Contaminant Hydrogeology, Prentice Hall, Upper Saddle River, NJ, 1992.

[39] C.D. Langevin, W.B. Shoemaker, W. Guo, Modflow-2000, The US Geological Survey Modular Groundwater Model--Documentation of the SEAWAT-2000 Version with the Variable-Density Flow Process (VDF) and the Integrated MT3DMS Transport Process (IMT), Tallahassee, Florida, 2003.
[40] S. Al-Yaqoubi, Understanding Saline Water Dynamics in Coastal Aquifers Using Sand Tank Experiment and Numerical Modeling, In: Soils, Water, and Agricultural Engineering, M.Sc. Thesis, Sultan Qaboos University, Sultanate of Oman, 2020.
[41] A. Abdoulhalik, A.A. Ahmed, How does layered heterogeneity affect the ability of subsurface dams to clean up coastal aquifers contaminated with seawater intrusion?, J. Hydrol., 553 (2017) 708–721.